Journal of Palaeogeography, 2023, 12(1): 107–128 (00290)

Available online at www.sciencedirect.com

ScienceDirect

journal homepage: http://www.journals.elsevier.com/journal-of-palaeogeography/

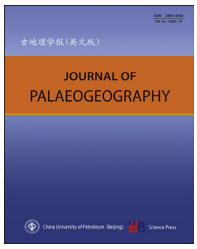

Lithofacies palaeogeography and sedimentology

Sedimentary–tectonic interaction on the growth sequence architecture within the intraslope basins of deep-water Niger Delta Basin

Jia-Jia Zhang [a,*], *Sheng-He Wu* [a], *Guang-Yi Hu* [b], *Da-Li Yue* [a], *Cheng Chen* [b], *Mei Chen* [a], *Ji-Tao Yu* [a], *Qi-Cong Xiong* [a], *Li-Qiong Wang* [c]

[a] *College of Geosciences, State Key Laboratory of Petroleum Resource and Prospecting, China University of Petroleum (Beijing), Beijing 102249, China*
[b] *Research Institute, China National Offshore Oil Corporation, Beijing 100028, China*
[c] *The Fourth Gas Production Plant, Changqing Oilfield Company, PetroChina, Ordos 017300, Inner Mongolia Autonomous Region, China*

Abstract This paper presents a 3D seismic-based case study from the deep-water Niger Delta Basin to investigate sedimentary–tectonic interaction on growth sequence architecture within the thrust-related intraslope or piggyback basins. Gravitational contraction in the lower continental slope had yielded a series of thrust faults and associated folds in the study area, which formed several piggyback basins. These basins were filled by a suite of growth sequences with varying stratigraphic architecture. Analysis of the 3D seismic data recognized three primary seismic facies types respectively as: convergent, draping and chaotic, which contain seven subtypes. These facies types are combined to form different filling successions for convergent or chaotic growth sequences. The convergent growth sequences mainly occur in the deep section of basin fills during strong gravitational deformation, and always began with convergent-baselapping strata succeeded by convergent-thinning strata, representing pond-to-bypass transition in the ponded-basin accommodation space. The chaotic growth sequences mainly occur in the shallow section of basin fills in response to weak gravitational deformation, and usually began with debris-flow deposits succeeded by channel-levee complexes, reflecting dominant erosion-bypass processes in the slope accommodation space. A dynamic fill-and-spill model considering relationship between episodic sedimentation rate and structural growth rate is proposed to explain the formative mechanisms of growth strata units and associated successions. Interaction between glaciation or deglaciation and sea-level change and gravitational deformation history are suggested to be the factor which resulted in the complex stratal stacking patterns, including progradational or retrogradational stacking patterns within convergent growth sequences, and progradational stacking patterns within chaotic growth sequences.

* Corresponding author.
E-mail address: zhangjiajia0103@cup.edu.cn (J.-J. Zhang).
Peer review under responsibility of China University of Petroleum (Beijing).
https://doi.org/10.1016/j.jop.2022.11.001

Keywords Intraslope basin, Gravitational deformation, Growth sequence, Stratigraphic architecture, Niger Delta Basin

Received 31 July 2022; revised 13 September 2022; accepted 13 September 2022; available online 12 November 2022

1. Introduction

Intraslope basins are widely developed in the continental slope setting resulting from a variety of tectonic mechanisms, such as salt or shale tectonics (e.g., Gee and Gawthorpe, 2006; Duerto and McClay, 2011; Galindo and Lonergan, 2020), and gravity-driven structures (e.g., Brown *et al.*, 2004; Jolly *et al.*, 2016). Growth strata associated with intraslope basins have been research hotspots as these strata can indicate the evolution history of intraslope basins. Previous studies have focused on the growth sequence architecture within the salt-withdrawal minibasins, especially in the Gulf of Mexico and Angola—Gabon Basin (e.g., Prather *et al.*, 1998; Brun and Fort, 2004; Madof *et al.*, 2009; Sylvester *et al.*, 2015; Curry *et al.*, 2018), which have revealed varying geometries of growth strata in response to the tectonic deformation of mobile salt substrates. Comparatively, studies on the growth sequence architecture within the thrust-related intraslope basins are much less.

The Niger Delta Basin is a classical shale tectonic province where gravity-driven fold and thrust belts are widely developed in the deep-water region (Fig. 1A, after Wu *et al.*, 2015), yielding a series of piggyback-style intraslope basins (Fig. 1B). Previous work in the deep-water Niger Delta Basin had emphasized structural control on the morphology of submarine fan-channel systems (e.g., Clark and Cartwright, 2011, 2012; Jolly *et al.*, 2016, 2017), but it is still poorly studied regarding the growth sequence architecture within the thrust-related piggyback basins. Unlike mobile salt substrates in other areas, shale substrate has lower mobility with weaker ductile deformation under deeply-buried setting, which can make big differences in the growth sequence architecture. Gravity-driven deformation along basal shale detachment levels is considered to be the major driving force creating accommodation space in the piggyback basins, while gravity-flow sediment supply is determined by cyclic evolution of shelf-edge sedimentary systems. Thus, the growth sequence architecture within piggyback basins serves as a proxy indicating the spatio—temporal interaction between deep-water sedimentation and growing structures. One main objective of this study is to reveal the effects of sedimentary—tectonic interaction on the distinctive growth sequence architecture associated with thrust-related intraslope basins, which complements existing stratigraphic models from the salt-withdrawal minibasins.

This study focuses on a gravity-driven fold and thrust system in the deep-water Niger Delta Basin, which resulted in several piggyback basins overlain by thick growth sequences (Fig. 1B). By 3D-seismic characterization of growth sequence architecture, this study addresses two key questions on the thrust-related intraslope basins: 1) how the growth strata units have been formed synchronously with the thrust-related folding and where the difference lies from the salt tectonics; 2) what kind of representative growth sequence patterns applies to the thrust-related intraslope basins underlain by shale detachment units. The role of sedimentary—tectonic interaction is highlighted in the stratigraphic records, which improves the theory of deep-water sequence stratigraphy and provides guidance for the deep-water hydrocarbon exploration.

2. Geological background

The study area (~1200 km^2) is located in the southern lobe of the deep-water Niger Delta Basin where contractional thrusts and folds are extensively developed (Fig. 1A). The Niger Delta Basin was formed by the break-up of Gondwana during Early Cretaceous times (Uchupi, 1989), and by late Eocene the basin has gradually entered into drifting stage with the delta largely built across the passive margin until today. A nearly 12-km thick sediment wedge was formed covering an area of ~140,000 km^2 from subaerial fluvial delta to the associated submarine fan-channel systems (Cohen and McClay, 1996; Briggs *et al.*, 2006). The post-Paleocene deltaic succession consists of three diachronous lithological formations named the Akata Formation, Agbada Formation, and Benin Formation, which transitioned from prodelta marine shales to delta

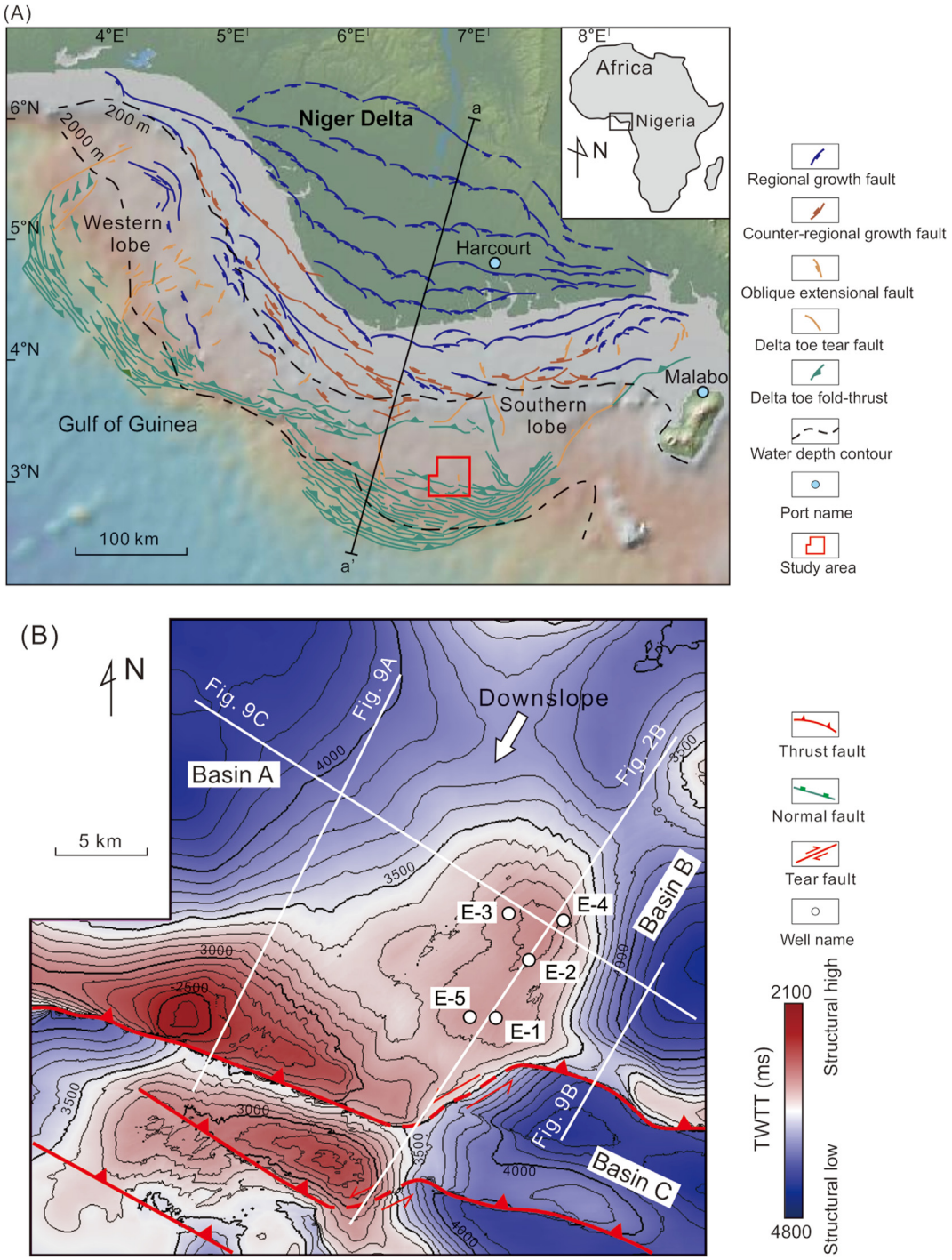

Fig. 1 **A)** Regional geological map of the Niger Delta Basin showing distribution of gravity-driven structural domains across the basin, after Wu *et al.* (2015). The study area is located in the southern lobe of the Niger Delta, structurally between the translational and compressional regions; **B)** Time-structure map of the basal boundary of syngrowth section (see Fig. 2B for the cross-sectional position of the boundary), showing gravitational structures and associated intraslope basins in the study area. The western fold-thrusts and eastern fold-thrusts are laterally linked by strike-slip tear faults, and separated by a central shale-detachment fold. These structures formed three major thrust-related intraslope basins, namely basin A, basin B, and basin C. The white solid lines represent the position of seismic profiles shown in the following description. TWTT = Two-way travel time.

front—submarine clastic deposits, and continentally sourced sands onshore (e.g., Corredor *et al.*, 2005). In the distal parts of the Niger Delta Basin, the Neogene deep-water clastic systems of Agbada Formation overlie the thick, overpressured, marine shales of Akata Formation. Gravitational collapse driven by the

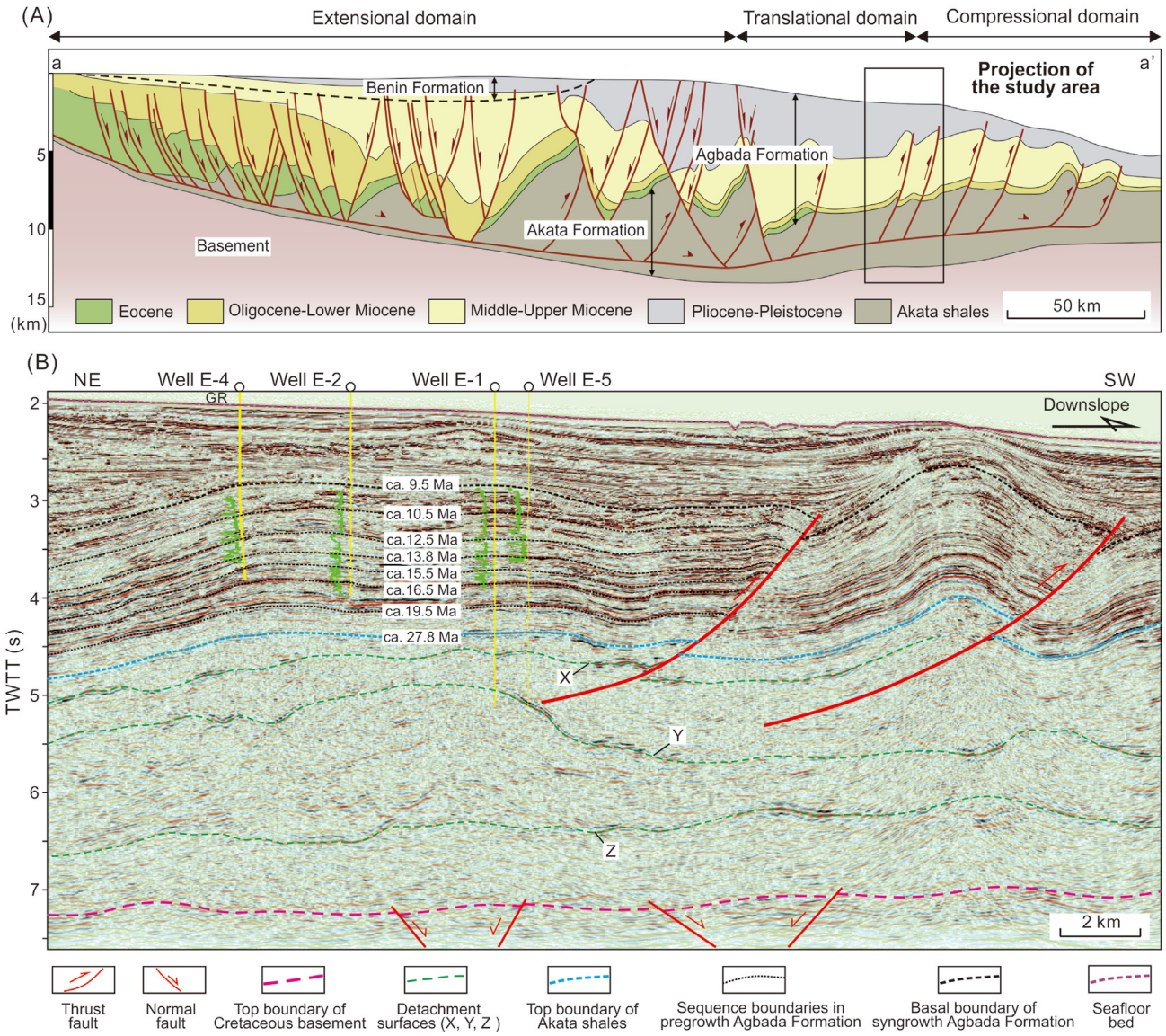

Fig. 2 **A)** Regional cross section of the Niger Delta Basin (see a—a' in Fig. 1A for the section position) showing stratigraphic distribution and gravity-driven structures across the basin, after Wu *et al.* (2015); **B)** Well-calibrated seismic profile (see Fig. 1B for the position of seismic line) showing tectono-stratigraphic features across the study area. The Akata shales contain three major detachment levels, namely X, Y, and Z. The overlying Agbada Formation can be divided into two parts of (pregrowth and syngrowth) intervals. TWTT = Two-way travel time.

prograding delta took place along multiple detachment levels within the mobile Akata shales (Fig. 2B), resulting in structural translation from extensional zone in the shelf—upper slope region to contractional zone in the lower slope—basin floor region (Fig. 2A). The Agbada Formation in the study area has undergone prominent thrusting and folding since ca. 9.5 Ma (Pizzi *et al.*, 2020; Zhang *et al.*, 2021), and consists of a lower pregrowth section and an upper syngrowth section (Fig. 2B). This study focuses on the sequence architecture of the upper syngrowth section which was filled within the thrust-related intraslope basins created by the synchronous gravitational deformation.

Previous work in the study area has revealed the tectono-stratigraphic features of the piggyback basins (Fig. 2B, after Zhang *et al.*, 2021). The structural styles consist of two sets (eastern and western) of thrust-propagation folds and a central detachment fold, involving prominent deformation in both the overburden of Agbada Formation and the basal Akata shales (Fig. 1B). These folds formed three piggyback basins (basin A, basin B, and basin C), where basin A and basin B are two major basins filled with thick, convergent, syngrowth strata (Fig. 3A). Eight growth sequences (GS1—GS8), roughly corresponding to third-order sequences, have been identified based on

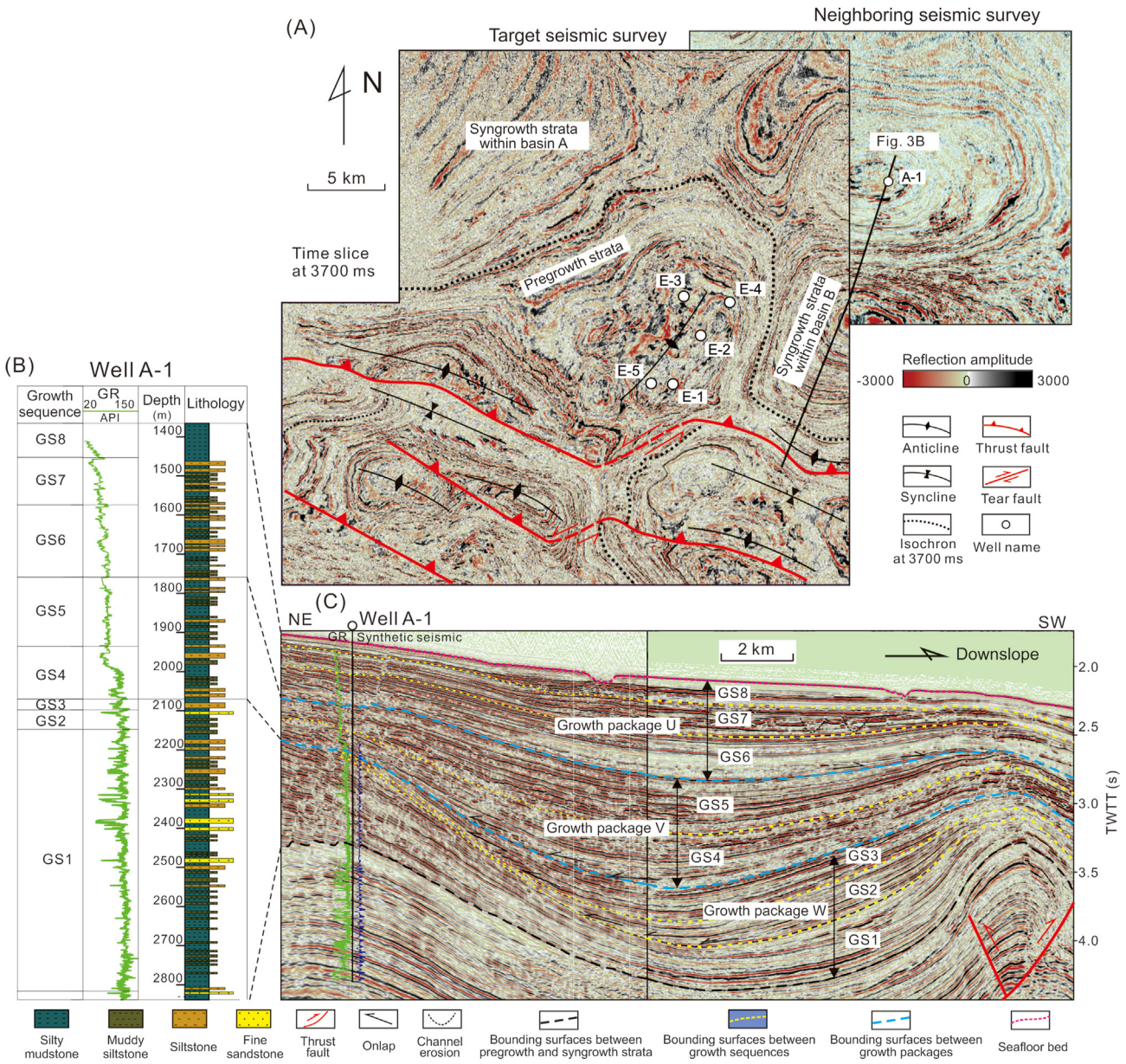

Fig. 3 **A)** Seismic time slice at 3700 ms TWTT showing distribution of syngrowth strata in the piggyback basins. The syngrowth strata within basin A and basin B display convergent reflections distinguished from the parallel reflections of pregrowth strata. The black dash line indicates the contour line of 3700 ms from Fig. 1B. The target seismic survey overlaps partially with the neighboring seismic survey; **B)** Drill bore column of Well A-1 from the neighboring seismic survey showing lithologic composition of the syngrowth strata. It features fine-grained sediments consisting of fine sandstones, siltstones, muddy siltstones and silty or pure mudstones. The interval with higher frequency of sands and silts corresponds to stronger seismic reflections; **C)** Seismic profile (see Fig. 3A for the position of seismic line) correlated with the neighboring seismic survey and well, showing the division of three growth strata packages (W, V, U) and eight growth sequences (GS1—GS8) within the thrust-related intraslope or piggyback basins. Varying geometries, seismic reflections and depocenters characterize the growth sequence architecture. TWTT = Two-way travel time.

unconformities near the basin margin and abrupt changes of seismic/well-log facies across the sequence boundaries (Fig. 3B and C). These growth sequences form three growth strata packages W, V, and U (Fig. 3C) proposed by Maloney *et al.* (2010), which amount to second-order sequences. Isochron maps of each growth sequence have revealed three tectonic evolution stages since the beginning of contractional deformation at ca. 9.5 Ma (Fig. 4, modified from Zhang *et al.*, 2021). The first stage dominated by thrust-propagation folding (deposition of GS1—GS3, Fig. 4A—C) was followed by the second stage of

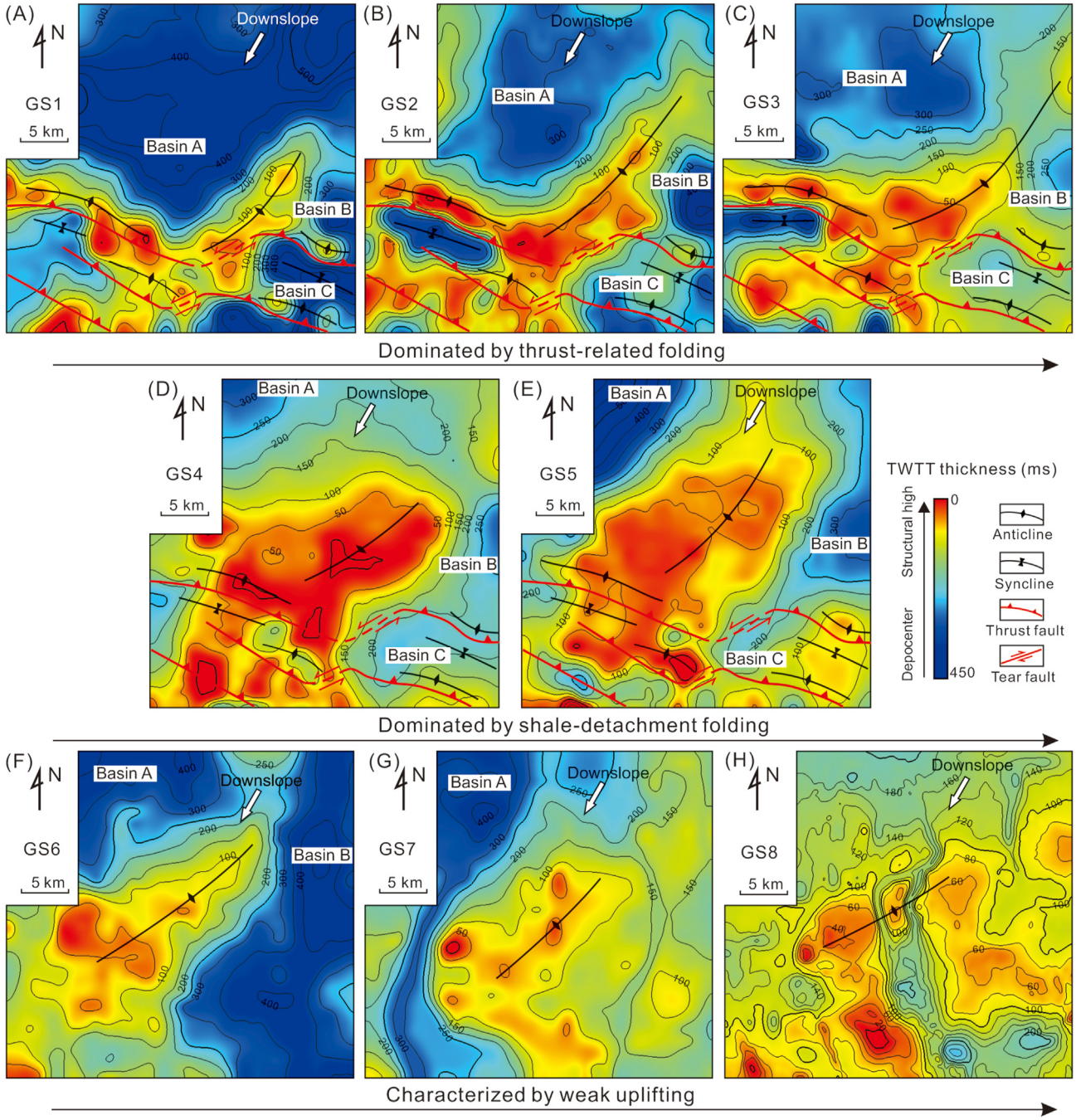

Fig. 4 Isochron maps for each growth sequence showing evolution of fold-thrust belts and associated piggyback basins, modified from Zhang *et al.* (2021). **A)**, **B)** and **C)** represent the first stage dominated by thrust-related folding; **D)** and **E)** represent the second stage dominated by shale-detachment folding; **F)**, **G)** and **H)** represent the third stage characterized by weak uplifting. The shape and scale of each basin vary significantly with the evolution of gravity-driven structures. The long black arrows under the three groups of isochron maps of each growth sequence represent an increase in sequences (from GS1 to GS8).

dominant detachment folding (deposition of GS4—GS5, Fig. 4D and E), and the overall folding activity waned greatly in the finale stage (deposition of GS6—GS8, Fig. 4F—H) (Maloney *et al.*, 2010; Zhang *et al.*, 2021). This structural evolution is controlled by the regional gravity-driven contraction and shale deformation along basal detachment surfaces (Fig. 2, see Zhang *et al.*, 2021 for the tectonic mechanism). The thrust-related folding provided effective accommodation space to trap large amount of sediment gravity flows and form thick growth sequences with varying stratigraphic architecture.

3. Accommodation space type of the study area

Understanding the concept of accommodation space is the basis for our following description of depositional process associated with intraslope basins. Two parts of accommodation space are included: 1) the lower part of ponded-basin accommodation space confined by the structural spill point; 2) the upper part of slope accommodation space confined by the slope equilibrium profile (Fig. 5). The ponded-basin accommodation space is the space created by the thrust-related folding, which can inhibit sediment transport and facilitate sediment deposition within the basin. At the top of the ponded-basin accommodation space is the slope accommodation space where sediments bypass and accumulate toward the slope equilibrium profile. Ratio between the ponded-basin accommodation space and slope accommodation space is connected to the intensity of thrust-related folding. Strong folding tends to result in dominance of ponded-basin accommodation space (Fig. 5A), while weak folding will result in dominance of slope accommodation space (Fig. 5B). The depositional processes will change in response to the evolution of accommodation space, forming complex growth sequence architecture.

4. Data and methodology

The primary data used in this study is a poststack time-migrated 3D seismic dataset, which has a bin size of 12.5 × 12.5 m and vertical sampling rate of 3 ms. The shallow section of syngrowth strata has a peak frequency of ~70 Hz, amounting to about 7 m vertical resolution calculated from an average strata velocity of

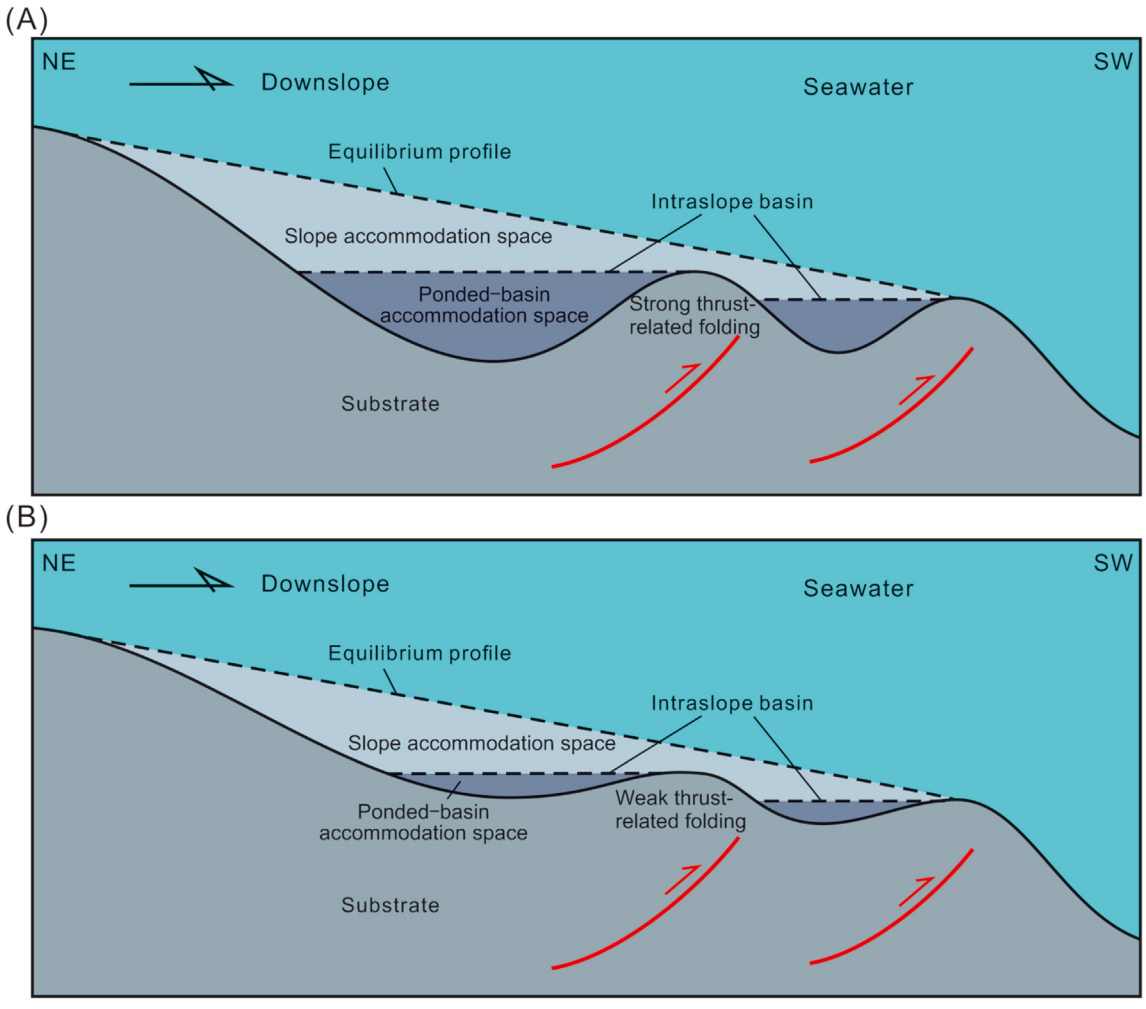

Fig. 5 Conceptual diagrams showing distribution of ponded-basin accommodation space and slope accommodation space associated with the thrust-related intraslope basins. **A)** is dominated by ponded-basin accommodation space due to strong thrust-related folding; **B)** is dominated by slope accommodation space due to weak thrust-related folding.

2000 m/s. The display of the volume is in "SEG normal polarity" with the peak reflectors representing downward increase in impedance. The seismic data were tied to Well A-1 from the neighboring seismic survey (Fig. 3B and C), which has well-logging records in both the pregrowth and syngrowth strata intervals and aids in lithologic calibration of seismic data across the study area. Seismic interpretation of growth strata units was based on the seismic facies analysis which considers the stratal feature (convergent/parallel, disconformity/conformity), seismic reflectivity (amplitude, continuity), and lithologic composition (sand/shale ratios). Seismic facies together with seismic attributes and isochron maps of growth sequence, were integrated to show the origin and distribution of growth strata units. Several growth strata units with genetic relationships were combined to form different filling successions of growth sequence. Through interpretation of several seismic profiles across different basins, differential stacking patterns of growth sequences were identified, which reflect the evolution of sediment supply with respect to accommodation space. The thickness ratio of growth strata units was quantitatively calculated and compared for each growth sequence, in order to indicate the continuous evolution of A/S (ratio between accommodation space and sediment supply).

5. Seismic data interpretation

5.1. Basic strata units within growth sequences

Our classification scheme of basic growth strata units refers to other descriptive schemes proposed for salt-related minibasins such as in the deep-water Gulf of Mexico (e.g., Prather *et al.*, 1998), but with differences in the interpretation of tectonic-depositional environment. Analysis of seismic facies integrating bounding surface type, seismic event configuration and reflectivity is conducted to characterize the varying growth strata geometries and lithologies. Three types of growth strata units are determined from the external strata geometry: 1) convergent, 2) draping, and 3) chaotic (Fig. 6), indicating different transporting-depositional processes associated with the evolution of the intraslope basins. Seven subtypes of growth strata units are further subdivided considering seismic reflection features including the internal reflection configuration and event continuity (Table 1; Fig. 6). The internal reflection configuration mainly differentiates baselapping strata from concordant strata in that they represent different intensity between sediment supply and growing structure. The term "baselap" used here is to eliminate the difficulty in discriminating onlap from downlap at the flanks of intraslope basins, which may transfer between each other due to structural inversion. The seismic reflectivity, calibrated by Well A-1 (Fig. 3B and C), indicates the lithological composition (sand/mud ratio) of the growth strata. High-amplitude reflections correlate to the serrated bell or funnel shape of gamma logs (GR), indicating sand-prone or mixed sand-mud units (interbedded sandstones, siltstones, and silty mudstones). Low-amplitude reflections correlate to mud-prone units dominated by silty or pure shales. This connection between seismic reflectivity and lithology in the syngrowth interval is consistent with the pregrowth interval calibrated by Well E−1 to Well E−5 (Fig. 2B). The variation of sand/mud ratio within a single growth sequence is considered to result from allogenic cycles of sediment supply. The details of main growth strata units are described as follows linking the seismic response, lithology and depositional environment (also see Table 1).

5.1.1. Convergent strata

Convergent strata are characterized by wedge-shaped strata thinning from the depocenters to the flanks of intraslope basins (Fig. 6A). Deposition of these convergent strata primarily took place in the ponded-basin accommodation space in response to strong tectonic uplifting at the flanks of basins, indicating strong interaction between sediment supplies and growing structures. Two subtypes are identified according to the bounding surface and internal reflection configuration: convergent-baselapping or convergent-thinning. Convergent-baselapping strata feature angular discordance at the flanks of basins, and manifest dominant high-amplitude, continuous reflectivity indicating high sand/mud ratios (Fig. 6A1). Convergent-thinning strata consist of concordant strata gradually thinning over the flanks of basins, and are dominated by low-amplitude, semi-continuous reflections indicating low sand/mud ratios (Fig. 6A2).

The convergent-baselapping highly reflective (Cbh) strata units mainly develop at the base of a single growth sequence and correspond to high-amplitude, lobate unit in map view (Fig. 7B), which are interpreted as sandy submarine lobe deposits ponded or trapped within the intraslope basins. The high accommodation space created by strong structural uplifting at basin margins facilitates the ponding of sand-prone sediment gravity flows at the beginning of a single growth sequence. The areal distribution of ponded submarine lobes is therefore controlled by the size and shape of receiving basins (Fig. 7A). In addition

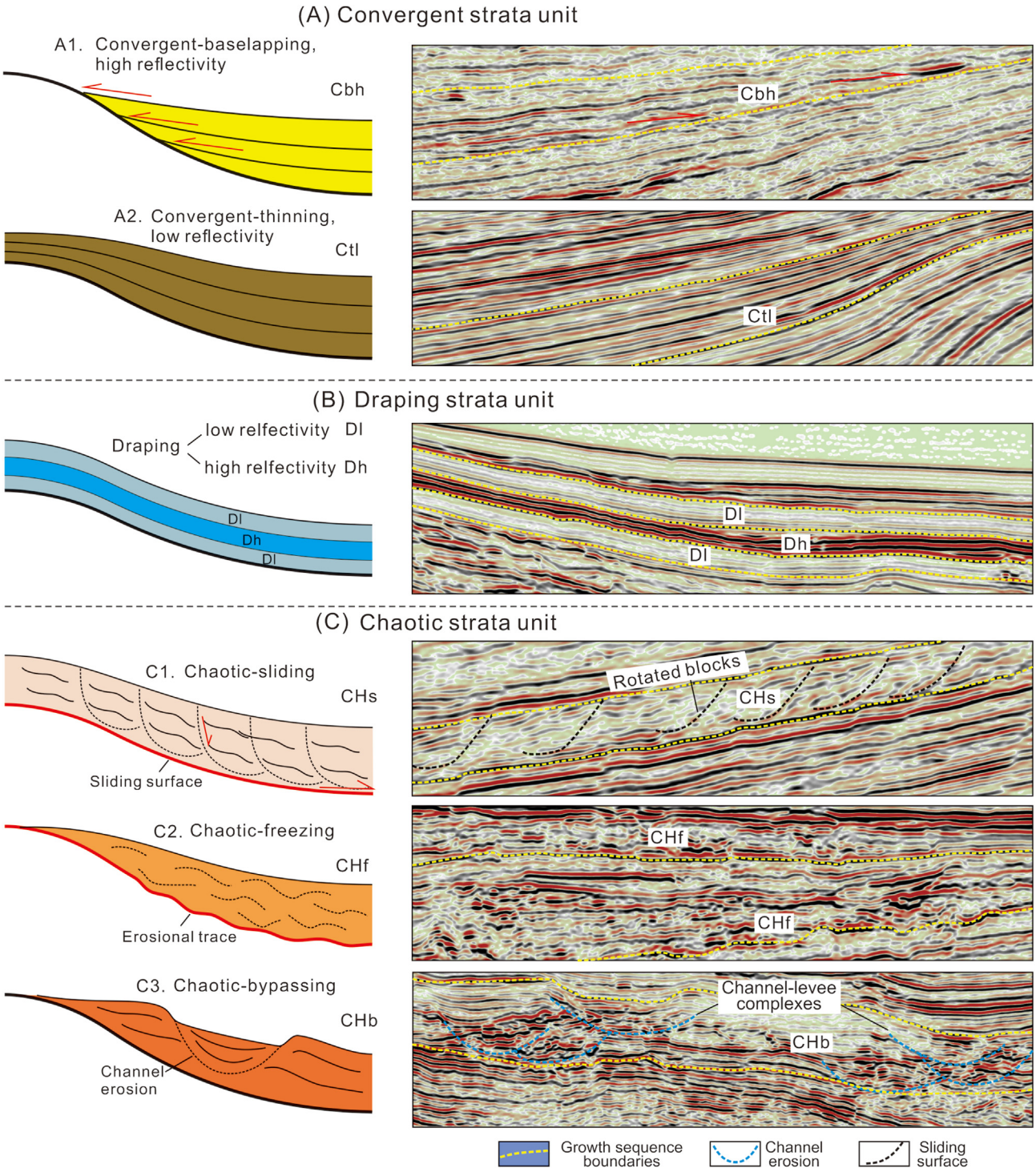

Fig. 6 Seismic-based classification of basic strata units within the thrust-related intraslope basins. **A)** Convergent strata unit consisting of convergent-baselapping (A1) and convergent-thinning (A2) subtypes; **B)** Draping strata unit with high and low reflectivity subtypes; **C)** Chaotic strata consisting of chaotic-sliding (C1), chaotic-freezing (C2), and chaotic-bypassing (C3) subtypes.

to allogenic factors (such as sea-level change) that control sand/mud ratios of sediment gravity flows, autogenic factors such as abrupt reduction in seafloor gradient or slope reversal at the hanging wall of thrust-related folds would result in formation of hydraulic jumps that could further prompt sand deposition (Lamb *et al.*, 2006). From the perspective of syntectonic deposition, the occurrence of baselapping discordance at basin margins suggests the sediment accumulation rate outpacing tectonic growth rate.

Table 1 Summary of basic growth strata units within the thrust-related intraslope basins.

Types and subtypes of growth strata units		Seismic characteristics	Lithology	Sedimentary system	Genetic mechanism	Sedimentary process	Distribution
Convergent strata	Convergent-baselapping, high reflectivity (Cbh)	Sheet-like reflections, wedge shape with baselapping near basin margin	Sheet-like sandbodies intercalated with shales	Sand-prone lobe systems	Dominated by high-density turbidities	Sediment ponding	At the base of a single growth sequence, commonly in the deeper GS1—GS5
	Convergent-thinning, low reflectivity (Ctl)	Subparallel reflections with gradual thinning toward basin margin	Interbedded sands and shales, containing local channelized sands	Mud-prone systems of overbanks and associated channels	Dominated by low-density turbidities	Sediment bypassing	In the upper part of a single growth sequence, commonly in the deeper GS1—GS5
Draping strata	Draping, low reflectivity (Dl)	Low-amplitude or transparent reflections with uniform thickness	Organic-rich shales	—	Hemipelagic shales	Vertical fallout	At the top of a single growth sequence
	Draping, high reflectivity (Dh)	High-amplitude, high-continuity reflections, slightly thinning toward basin margin	Interbedded clays and silts	—	Hemipelagic shales and muddy turbidites	Vertical fallout and sediment bypassing	At the top of a single growth sequence, usually in the shallower growth sequences
Chaotic strata	Chaotic-sliding (CHs)	Low-amplitude, discontinuous reflections with internal faulting, featuring rotated blocks with erosional base	Interbedded fine-grained sands, silts, and clays	Intrabasinal mass-transport deposits (MTDs)	Sliding of muddy sediments along basin margin	Sliding of mud-prone sediments	In the upper part of a single growth sequence, mainly in the deeper GS2—GS3
	Chaotic-freezing (CHf)	Low-amplitude, wavy to chaotic reflections with erosional base	Mélange of conglomerates, sands and silts in muddy matrix	Extrabasinal MTDs	Muddy debris flows	Freezing of mud-prone sediments	At the base of a single growth sequence, commonly in the shallower GS6—GS8
	Chaotic-bypassing (CHb)	Moderate to high reflectivity, dominated by U-shaped units	Varied lithologies, channelized sands intercalated with fine-grained sediments	Channel-levee systems	High- to low-density turbidites	Sediment bypassing	In the upper part of a single growth sequence, commonly in the shallower GS6—GS8

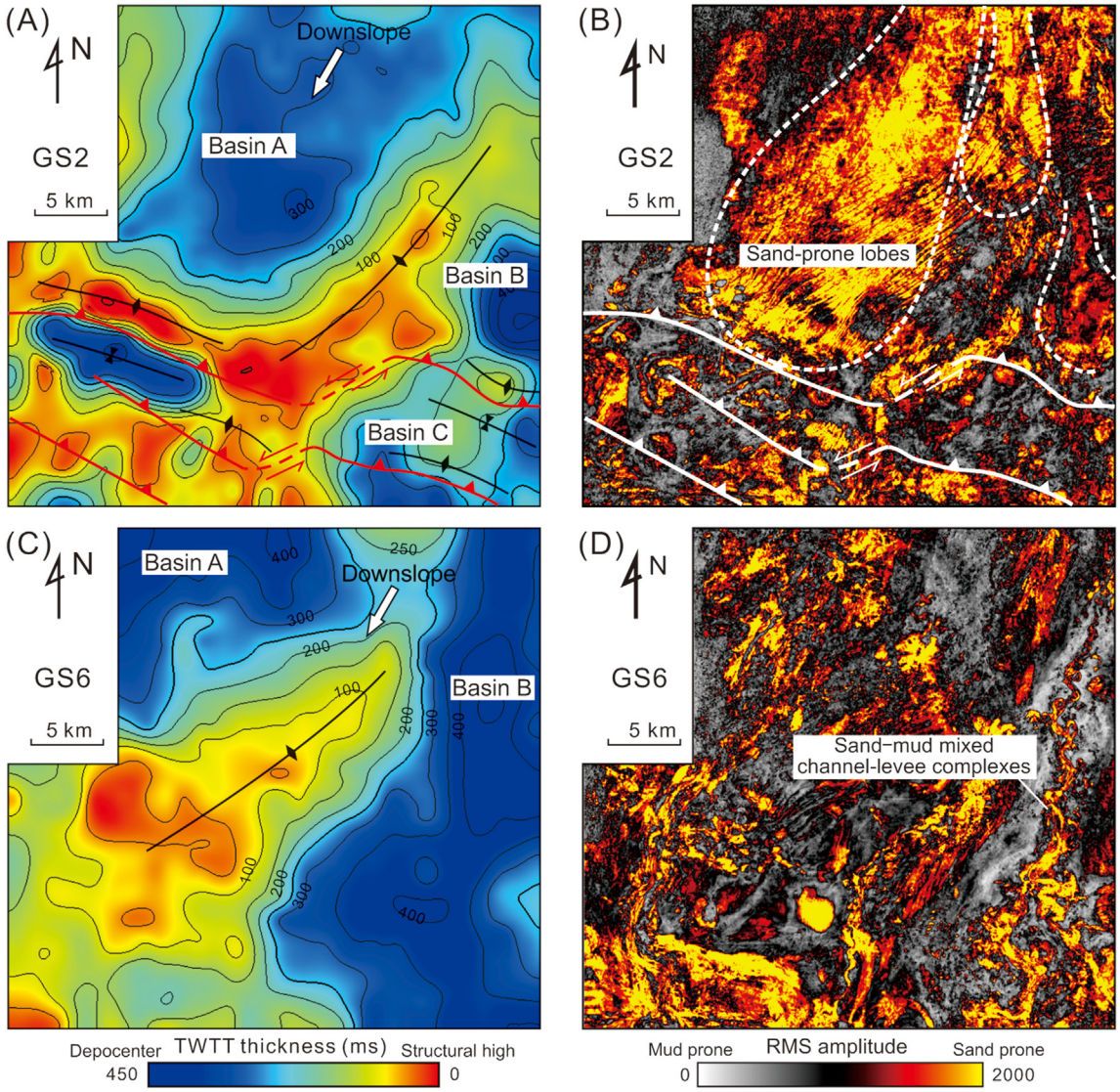

Fig. 7 Comparison between isochron maps (**A** and **C**) and root-mean-square (RMS) amplitude maps (**B** and **D**) showing distribution of different growth strata units. **A)** and **B)** indicate sand-prone lobes (Cbh) deposited within the ponded-basin accommodation space during the deposition of GS2. **C)** and **D)** indicate sand—mud mixed channel—levee complexes bypassing through the slope accommodation space during the deposition of GS6.

The convergent-thinning lowly reflective (Ctl) strata units, mainly developed in the upper part of a single growth sequence, are interpreted as muddy overbank deposits from aggradational channels bypassing through the ponded basins. The gentle reduction in seafloor gradient together with mud-prone sediment gravity flows aided in the development of several small-scale bypassing channels associated with the Ctl strata, which transported large amounts of gravity-driven sediments further downslope with muddy suspensions overspilled across the intraslope basins. The suspended clays and silts can be carried by the momentum of the flow over the flanks of basins, where the sediment accumulation rate amounts to the tectonic growth rate which caused the formation of Ctl strata.

5.1.2. Draping strata

Draping strata are characterized by a set of parallel reflections that drape evenly from basin depocenters to basin flanks with no convergence (Fig. 6B). The nearly uniform thickness distribution across the intraslope basins suggests a major component of passive fallout of hemipelagic shales that host similar accumulation rate over paleotopography. Seismic reflectivity differentiates two draping subtypes: draping lowly reflective (Dl) strata or draping highly reflective

(Dh) strata. The Dl strata mainly develop at the top of a single growth sequence, and their low-amplitude or transparent reflections indicate a pure shale interval without notable impedance difference, characteristic of the dominant hemipelagic deposition formed at sea-level highstands. In contrast, the Dh strata are characterized by high-amplitude, high-continuity, and high-frequency reflections with slightly thinning trend toward the basin margins. These features, as calibrated by Well A-1 (Fig. 3B), correspond to a combination of hemipelagic shales and low-density turbidite clays and silts that result in high impedance difference and high reflectivity. The two draping strata units are overall dominated by hemipelagic shales formed during inactive periods of sediment gravity flows, and the Dh mainly develops in the shallow growth sequences (GS6—GS8), which might look similar to the Dl in the deeper growth sequences (GS1—GS5) as the seismic resolution decreases downward.

5.1.3. Chaotic strata

Chaotic strata are characterized by wavy or discontinuous reflections with variable reflectivity (Fig. 6C), which indicate complex erosional—depositional processes with internal deformations. Three chaotic subtypes are recognized based on internal reflection configuration and reflectivity: chaotic-sliding (CHs), chaotic-freezing (CHf), and chaotic-bypassing (CHb) (Fig. 6C1—C3). The occurrence of rotated blocks characterizes the CHs strata, distinguishing from other two subtypes (CHf, CHb) that are differentiated by seismic reflectivity. These chaotic strata units reflect different process regimes associated with different types of sediment gravity-flows.

CHs strata mainly occur on the basin margins with several rotated blocks sliding toward the basin depocenters (Fig. 6C1), representing gravity-driven sliding processes. Small-scale normal faults internal to the CHs strata adjoin upon a common basal detachment surface, usually along the draping strata. The overall low reflectivity indicates low sand/mud ratios similar to the Ctl strata. These mud-prone units originally from low-density turbidity currents are incompetent rocks that are easily subjected to sliding deformations in response to strong structural uplifting near the basin flanks. Therefore, CHs strata represent intrabasinal mass-transport deposits (MTDs) induced by basin tectonics (e.g., Madof *et al.*, 2009). Several CHs strata may stack locally indicative of high structural growth rate as the deposition of sediment gravity-flows took place synchronously.

CHf strata mainly occur at the base of a single growth sequence, usually in the shallow growth sequences (GS6—GS8). The common erosional bases together with low-amplitude, wavy reflections (Fig. 6C2) suggest an origin of muddy debris-flows, which could strongly erode underlying strata in the downslope-transporting process and become rapidly frozen with the decreasing of velocity. Several sands may be trapped in the ductile muddy matrix due to rapid freezing of variable-grained gravity flows. Differing from the intrabasinal-sliding CHs strata, the CHf strata are mainly distributed at basin depocenters with tiers of erosional traces at the base. This feature suggests the extrabasinal origin for muddy debris-flows deposits, which might form in response to the early forced regression of sea level (e.g., Zecchin and Catuneanu, 2013). In the continental setting, deposition of muddy debris flow normally took place further upstream of high-density turbidity currents (Postma *et al.*, 1988), usually in the slope accommodation space of intraslope basins where erosion easily happened.

CHb strata mainly stack over the CHf strata, and are characterized by a complex set of U-shaped reflection units (Fig. 6C3) corresponding to sinuous channel-levee complexes in map view (Fig. 7). The overall high reflectivity within the channels indicates sand-prone or mixed sand-mud channel fills, whereas the low reflectivity on the channel flanks or inter-channel environments indicates mud-prone levee or overbank deposits. Deep-water channels are considered as a significant sediment transporting regime on the continental slope (e.g., Deptuck *et al.*, 2008; Mchargue *et al.*, 2011; Janocko *et al.*, 2013; Damuth and Olson, 2015). Extensive development of deep-water channels (CHb) in the shallow growth sequences (GS6—GS7, Fig. 7D) suggests the dominant bypassing of sediments through intraslope basins (Fig. 7C), distinct from the dominant ponding of sediments indicated by convergent strata in the deeper growth sequences (GS1—GS5, Fig. 7A and B). Unlike the Ctl strata that may contain small channels winding around the basin flanks, the CHb strata consist of large constructive channels crossing over the basin flanks, which suggests that the sediment accumulation rate significantly outpaced the structural growth rate.

5.2. Filling successions of growth sequences

The filling successions of single growth sequences consist of several related strata units. Predominance of different growth strata units differentiates two types of sequence successions: convergent or chaotic filling successions. These two filling successions potentially reflect different evolution phases of the thrust-controlled intraslope basins.

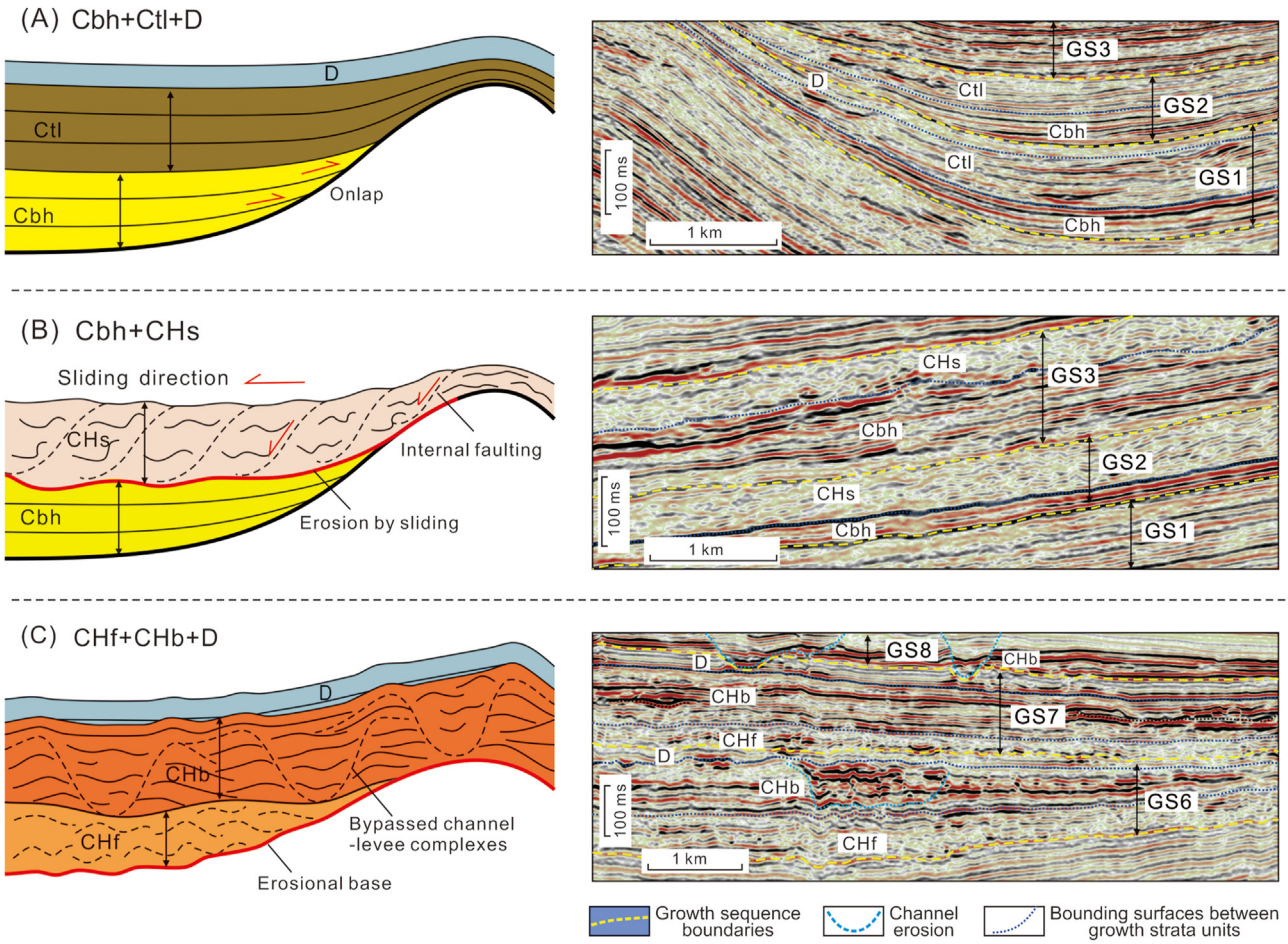

Fig. 8 Filling successions within single growth sequences. **A)** and **B)** are convergent filling successions characterized by sediment ponding (Cbh) at the start of growth sequences; **B)** differs from **A)** by the sliding of chaotic blocks (CHs) in the upper part of growth sequences; **C)** Chaotic filling successions dominated by sediment bypassing (channel-levee complexes, CHb) in the slope accommodation space. Dashed lines in yellow are sequence boundaries identified by unconformities near the basin margin and abrupt changes of seismic/well-log facies across the sequence boundaries.

5.2.1. Convergent filling successions

Convergent filling successions mainly occur in the deep growth sequences (GS1—GS5), which are dominated by Cbh, Ctl or CHs, and Dh or Dl strata units (Fig. 8A and B). Strata upward-shallowing or strata rotation near basin flanks is characteristic of convergent filling successions, suggesting synchronous interaction between deep-water sedimentation and gravity-driven thrusting. Common occurrence of Cbh strata at the base of single growth sequences indicates dominant ponding of sandy sediments in the early highly-confined intraslope basins. It was succeeded by Ctl strata as the gravity-driven sediment supply decreased, indicative of bypassing of muddy sediments (Fig. 8A). The transition from Cbh to Ctl strata mainly took place in the ponded-basin accommodation space created by strong thrust-related folding (see Fig. 5A), and reflects ponded-to-bypass transition associated with sedimentary cycles. With this transition the sediment accumulation rate gradually decreased close to the structural growth rate at the flanks of basins. If the hanging wall of thrust-related folds experienced strong uplifting, the unconsolidated Ctl strata would be subjected to sliding or slumping deformation near the basin flanks, forming CHs strata (such as in GS2—GS3, Fig. 8B). Sometimes draping strata (D) can be recognized on the top of Ctl or CHs strata, representing fallout of hemipelagic shales at the end of growth sequences. As draping strata are much thinner with low sedimentation rate, it may be incorporated with the Ctl strata. Besides, erosion by subsequent gravity flows may lead to the lack of draping strata in several places.

5.2.2. Chaotic filling successions

Chaotic filling successions mainly occur in the shallow growth sequences (GS6—GS8), which are dominated by chaotic strata units (CHf or CHb) with minor draping strata (Dl or Dh). This type of succession always begins with CHf strata, succeeded by thick CHb strata and capped by thin Dl or Dh strata (Fig. 8C). Lack of strata rotation near the basin flanks suggests the overall weak structural activity, leading to a minimal component of ponded-basin accommodation space (see Fig. 5B). Thus, filling of intraslope basins mainly took place in the slope accommodation space. The basal CHf strata represent the muddy debris-flow deposition induced by the forced regression of sea level in early period. The CHf strata show strong erosive base with varied thicknesses, and may be absent in the latest GS8 due to the small slope accommodation space. Early deposition of CHf strata would result in a relatively gentle topography across the basins, which is conductive to the formation of large constructive channels in the overlying CHb strata. These channels, either strongly or weakly incising the older strata, can cross over the topographic confinement of intraslope basins and transport sediments further downslope (see Fig. 7C and D). This suggests dominant bypassing of sediments, with the sediment accumulation rate associated with channel-levees being significantly higher than the structural growth rate. The chaotic growth sequences also end with hemipelagic shales indicated by continuous draping strata. Overall, the chaotic filling successions reflect a complex erosion-bypassing process taking place in the slope accommodation space.

5.3. Evolution of growth sequence architecture

Three seismic lines crossing different piggyback basins and associated thrust-folds (Fig. 9A—C) were systematically interpreted to reveal the tempo-spatial evolution of growth sequence architecture. Results show that the deep growth sequences (GS1—GS5) are generally characterized by convergent filling successions with notable wedged shape and strata rotation, corresponding to the early phase of strong structural activity. Predominance of ponded-basin accommodation space (see Fig. 5A) facilitated capture of significant volumes of sediments within the basins, as indicated by the occurrence of Cbh at the base of each growth sequence. Comparatively, the shallow growth sequences (GS6—GS8) are characterized by chaotic filling successions with strong erosion and less strata rotation, corresponding to the late phase of weak structural activity. Gradual filling of the slope accommodation space (see Fig. 5B) is accompanied with sediment bypassing by large channel-levee systems (CHb). Overall, the growth sequence architecture experienced an upward change from convergent filling successions (GS1—GS5) to chaotic filling successions (GS6—GS8), with the dominant ponded-basin accommodation space (Fig. 5A) being replaced by dominant slope accommodation space (Fig. 5B). This evolution of growth sequence architecture reflects a larger stratigraphic scale of ponded-to-bypass transition (compared to the short-term transition from Cbh to Ctl within a single growth sequence) in response to the gradual waning of structural activity.

The evolution of growth sequence architecture is also expressed by the change in the proportion of strata units between growth sequences, which reflects varying stratigraphic stacking patterns associated with the change of A/S (ratio between accommodation space and sediment supply). As for the convergent filling successions, the thickness ratio of Cbh within a single growth sequence is an important parameter indicating the A/S of basins (accommodation space over sediment supply). Lower thickness ratio of Cbh generally indicates higher A/S ratio, implicating that the ponding of high-density turbidites was overwhelmed by subsequent bypassing of low-density turbidites. Here we calculated the thickness ratio of Cbh for each growth sequence in basin A and basin B (Table 2). From GS1 to GS3, the thickness ratio of Cbh increased upwards suggesting upward-decreasing A/S (Table 2; Fig. 9). This reflects a progradational stacking pattern for convergent strata, corresponding to the first stage characterized by weakening of thrust contraction. From GS4 to GS5, the upward-decreasing thickness ratio of Cbh indicates an upward-increasing trend of A/S. This reflects a retrogradational stacking pattern for convergent strata, corresponding to the second stage dominated by shale-detachment folding.

As for the chaotic filling successions, the thickness ratio of CHf strata and the degree of channel erosion in CHb strata indicate the change of slope accommodation space. From GS6 to GS8, the proportion of CHf strata decreased upwards, with the overlying CHb strata evolving from depositional channels to erosional channels (Fig. 9). This reflects a progradational stacking pattern for chaotic strata, due to the rapid filling of slope accommodation space. In this process, the slope topography became close to the slope equilibrium profile, and the stronger incision of channels provided additional accommodation space for sediment transporting. Additionally, difference exists in the chaotic strata features between the western and eastern piggyback basins (A and B), as influenced by

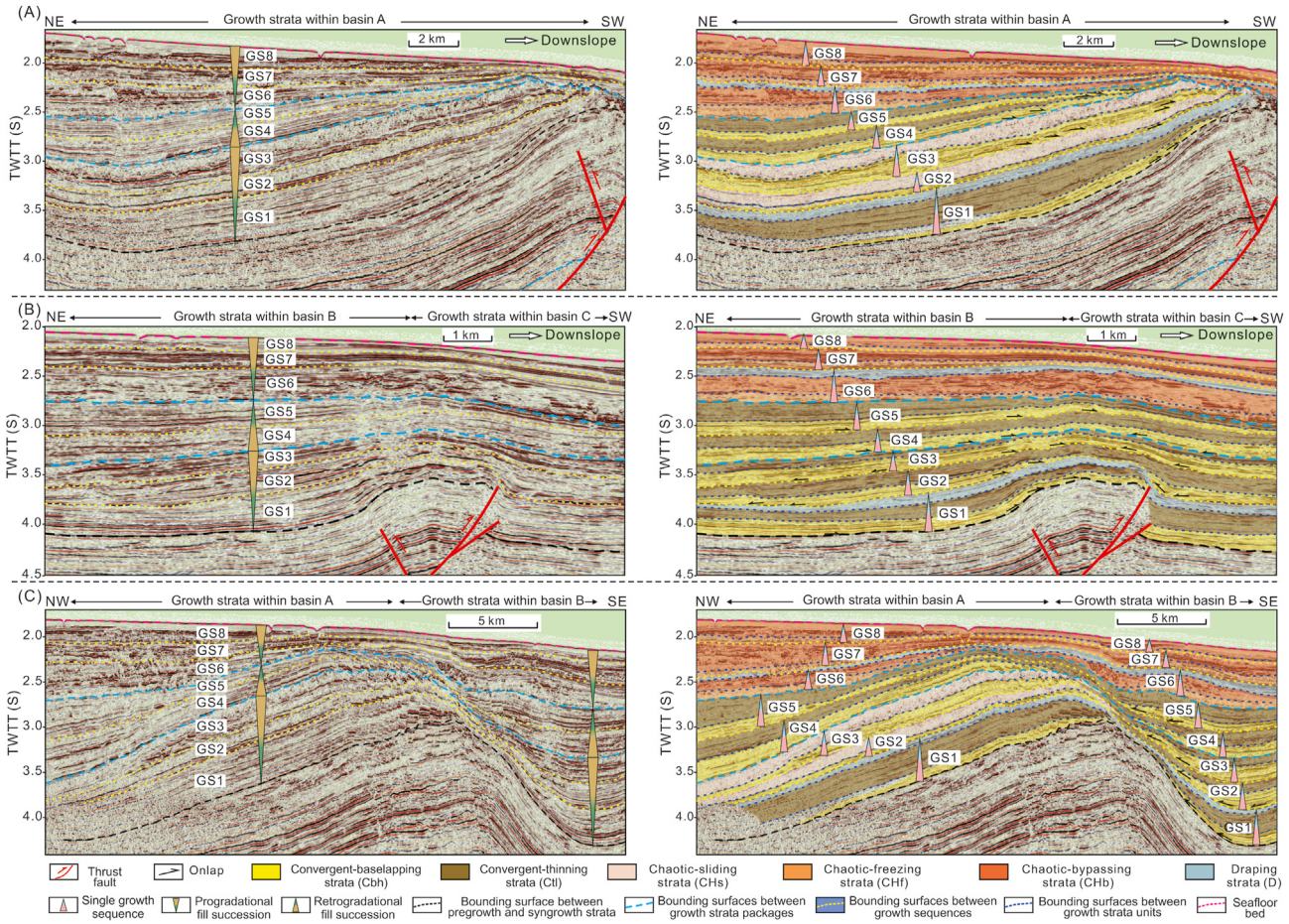

Fig. 9 Seismic profiles (see Fig. 1B for the position of seismic lines) and interpretations showing spatial distribution and evolution of growth sequence architecture. **A)** Dip seismic profile across the western fold-thrusts showing growth sequence architecture in basin A; **B)** Dip seismic profile across the eastern fold-thrusts showing growth sequence architecture in basin B and basin C; **C)** Strike-oriented seismic profile across the central detachment fold showing growth sequence architecture in basin A and basin B. Convergent filling successions representing progradational pattern characterize GS1—GS3. Convergent filling successions representing retrogradational pattern characterize GS4—GS5. Chaotic filling successions with progradational trend characterize GS6—GS8. TWTT = Two-way travel time.

the distribution of slope accommodation space. The western basin A is characterized by strongly incisive channels over the high topographic relief of thrust-related fold crest (Fig. 9A), where the slope accommodation space is minimal. The eastern basin B is characterized by dominant depositional channels over the lower topographic relief of thrust-related fold crest (Fig. 9B), where higher slope accommodation facilitated the development of aggradational channel-levee complexes.

Table 2 Thickness ratio of convergent-baselapping strata (Cbh) calculated for each growth sequence.

	Growth strata package W			Growth strata package V	
	Ratio of Cbh in GS1	Ratio of Cbh in GS2	Ratio of Cbh in GS3	Ratio of Cbh in GS4	Ratio of Cbh in GS5
Basin A	0.2	0.3	0.5	0.4	0.3
Basin B	0.4	0.6	0.7	0.5	0.4

6. Discussion

6.1. *Formative mechanisms of growth strata units and filling successions*

Our study reveals various growth strata units within growth sequences that constitute complex sequence-filling successions. The convergent strata units and associated filling successions are important growth strata records indicating syndepositional tectonic evolution. Analysis of growth axial polygon had been used to develop the kinematic models of thrust-related folds (e.g., Suppe, 1985; Corredor *et al.*,

2005). These models, however, are based on the assumption that the sedimentation rate is in equilibrium with the tectonic movement rate without notable topographic relief. In this study, the convergent growth sequence commonly beginning with base-lapping strata (Cbh) suggests the existence of topographic relief prior to sedimentation, i.e., thrusting activity led to development of intraslope basin that confined subsequent sedimentation.

Two different mechanisms have been proposed to illustrate the formation of convergent strata within intraslope basins. One is the static fill-and-spill mechanism that assumes constant ponded-basin accommodation space as sedimentation took place (e.g., Beaubouef and Friedmann, 2000; Li *et al.*, 2010). This situation is controlled by the sedimentary process itself, and the sediment spilling out of basins happened as basin filling reaches the structural spill point. The convergent stratigraphic architecture under the static mechanism features passive onlapping without strata rotation near basin flanks, and stacking of growth sequences generally lasts for a short period due to the rapid filling of accommodation space. Another is the dynamic fill-and-spill mechanism that assumes varied ponded-basin accommodation space in synchronous with sedimentation (e.g., Prather *et al.*, 2012; Sylvester *et al.*, 2015). Higher sedimentation rate with respect to structural growth rate will lead to sediment filling in basins with decreasing accommodation space, whereas lower sedimentation rate with respect to structural growth rate will lead to sediment spilling out of basins with increasing accommodation space. The convergent stratigraphic architecture under the dynamic model features notable strata rotation near basin flanks, and stacking of growth sequences can last for a long period because of regeneration of accommodation space. These features are characteristic of the deep growth sequences (GS1—GS5) in the study area, thus, the formation of thrust-controlled convergent strata can be interpreted by the dynamic fill-and-spill mechanism.

The convergent strata within thrust-related basins are similar to the salt-controlled convergent strata, which are thought to be representative of dynamic fill-and-spill mechanism. Mobile salt substrate can be easily deformed in response to sediment loading, resulting in rapid regeneration of accommodation space and recurrence of fill-and-spill cycles (e.g., Brun and Fort, 2004; Kopriva and Kim, 2015; Curry *et al.*, 2018). In comparison with salt-withdrawal mini-basins, thrust-related piggyback basins are driven by the regional gravitational contraction along basal detachment surfaces (see detachment surfaces X, Y, and Z in Fig. 2B), which have lower deformation rate with longer durations. During the deposition of a single growth sequence, the structural growth rate is considered as constant or with minimal change, while the sedimentation rate can change continuously in response to the episodic fluctuation of sea level, influencing the evolution of growth sequence architecture. Based on this consideration, we propose the formative mechanism of convergent growth sequence within the thrust-related intraslope basins (Fig. 10).

Four stages can be divided according to the relationship between sedimentation rate and structural growth rate: I) At the beginning of a single growth sequence, the sand-prone sediment gravity flows had larger sedimentation rate than the structural growth rate, resulting in the formation of Cbh strata unit at the base of growth sequences (Fig. 10A and B). This represents dominant sediment ponding within the intraslope basins, with the ponded-basin accommodation space decreasing gradually; II) As the sediment gravity flows became sand-mud mixed, the sedimentation rate decreased nearly close to the structural growth rate, resulting in the formation of Ctl strata unit overlying the Cbh strata (Fig. 10C). This represents the dominant sediment bypassing in intraslope basins, with minimal change in the ponded-basin accommodation space; III) Subsequently, the mud-prone sediment gravity flows had lower sedimentation rate than the structural growth rate, resulting in the formation of offlapping strata that are uneasy to recognize seismically due to their thin thickness and muddy lithology (Fig. 10D). The ponded-basin accommodation space started to increase during this stage; IV) At the end of the growth sequence, predominance of hemipelagic shales over sediment gravity flows made much lower sedimentation rate than the structural growth rate, resulting in the formation of draping strata and continued increase in the ponded-basin accommodation space (Fig. 10E). Overall, the former two stages characterized by higher sedimentation rate represent the basin-filling stage with gradual decrease in the ponded-basin accommodation space (Fig. 10F). The latter two stages characterized by lower sedimentation rate (higher structural growth rate) represent the basin-underfilling stage with gradual increase in the ponded-basin accommodation space. Longer duration of basin-underfilling potentially provides higher accommodation space prior to the deposition of younger growth sequence, which facilitates longer periods of stacking between growth sequences.

Differing from previous models, our model considers the evolution of sediment gravity flows and associated change of sedimentation rate during the formation of growth sequences; the resulting growth sequence architecture reflects both the transition in depositional

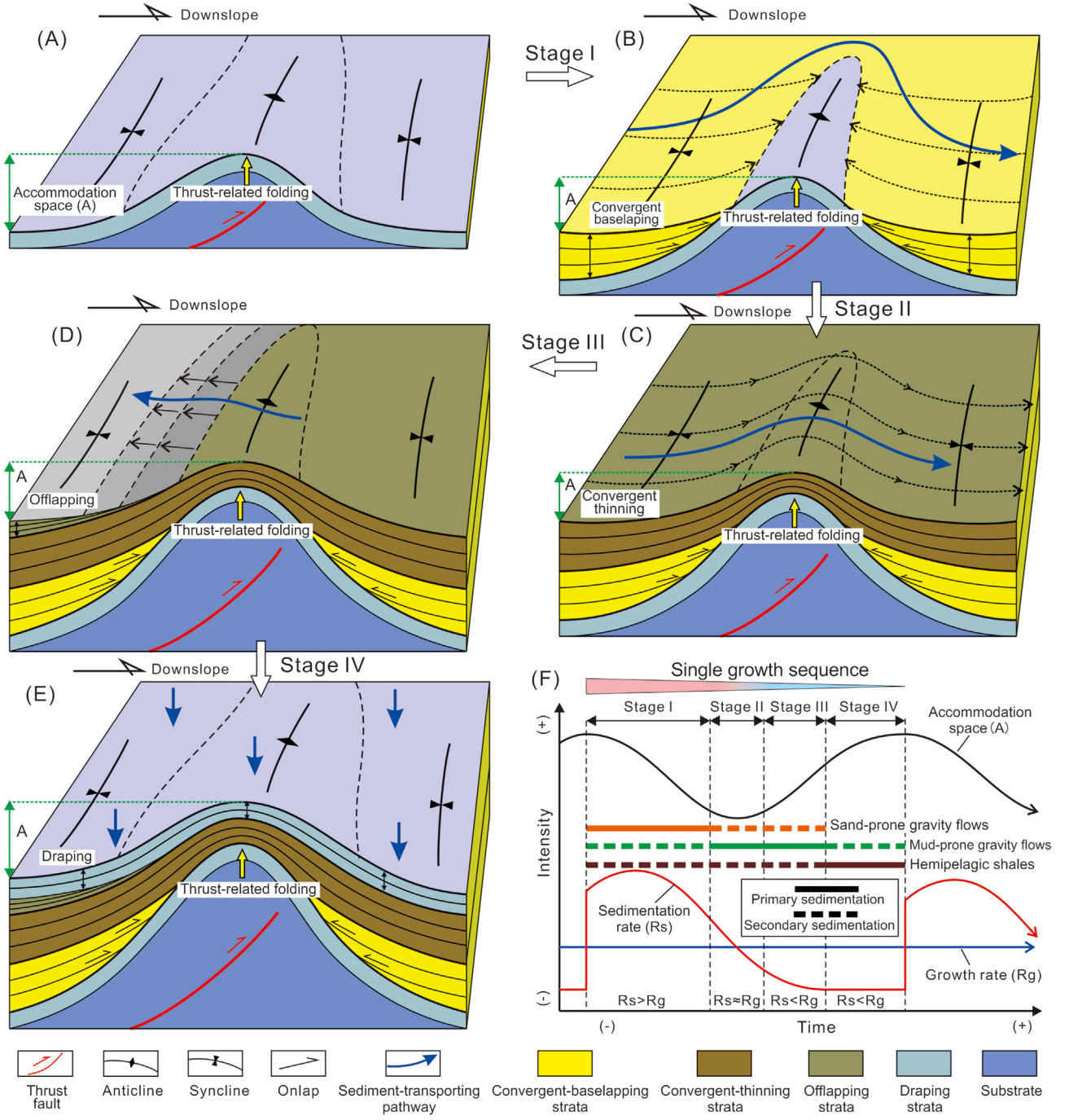

Fig. 10 Schematic illustration for the evolution of a single convergent growth sequence. **A—E)** Illustrations represent four-stage evolution from convergent-baselapping strata to convergent-thinning, offlapping, and draping strata; **F)** Idealized curves of the sedimentation rate (Rs), structural growth rate (Rg), and accommodation space during the evolution of a single growth sequence. The dominant types of sediment gravity flows evolve from sand-prone gravity flows to mud-prone gravity flows, and eventually form hemipelagic shales.

processes (ponding versus bypassing) and energies (sand versus mud), closer to the subsurface reality. Although the ponding to bypassing process occurring in the thrust-related piggyback basins is similar to that occurring in the salt-withdrawal minibasins, differences exist in the way of sedimentary—tectonic interaction. As the accommodation space of salt-withdrawal minibasins is created by the mobile deformation of salt substrate induced by sediment loading, the structural growth rate is closely related to the sedimentation rate. As for the thrust-related intraslope basins, the accommodation space is connected to the

regional gravity-driven contraction, and the structural growth rate is more independent from the cyclic variation of the sedimentation rate.

6.2. *Sedimentary—tectonic interaction on varying growth sequence architecture*

As discussed above, the development of growth strata units is closely related to the mutual relationship between the sedimentation rate and the structural growth rate. The sedimentation rate in the deep-water setting is largely driven by the regional sea-level change, while the structural growth rate is directly linked to the structural evolution in the study area. Thus, coupling between sea-level change and gravity-driven structural activity is assumed to result in the tempo-spatial evolution of growth sequence architecture.

Previous studies revealed that the studied intraslope basins had begun to develop since ca. 9.5 Ma, with thick growth sequences continuously filled until present day (e.g., Pizzi *et al.*, 2020; Zhang *et al.*, 2021). The global sea-level change curve had overall experienced a rising trend followed by a falling trend since ~9.5 Ma, and three stages could be recognized (Fig. 11). The first stage (~9.5 Ma — ~5 Ma) and the third stage (~3 Ma — 0 Ma) are characterized by overall low position of sea level with high-degree fluctuation, which represents the sea-level change under glacier condition. It is believed that large amounts of sediment supplies can be produced by the glaciation sea-level change, resulting in the extensive development of submarine-fan deposition in the deep-water setting (e.g., Gong *et al.*, 2016; Zhang and Gulick, 2020). The second stage (~5 Ma — ~3 Ma) is characterized by overall high position of sea level with low-degree fluctuation, representing the sea-level change under interglacial condition. Only a small amount of sediment supplies can be produced by the deglaciation sea-level change, resulting in the poor development of submarine-fan deposition in the deep-water setting (e.g., Gong *et al.*, 2016; Zhang and Gulick, 2020). According to Fig. 11, eight third-order falling—rising cycles of sea level can be recognized since ca. 9.5 Ma, during the same time eight growth sequences were deposited in the piggyback basins. Although we

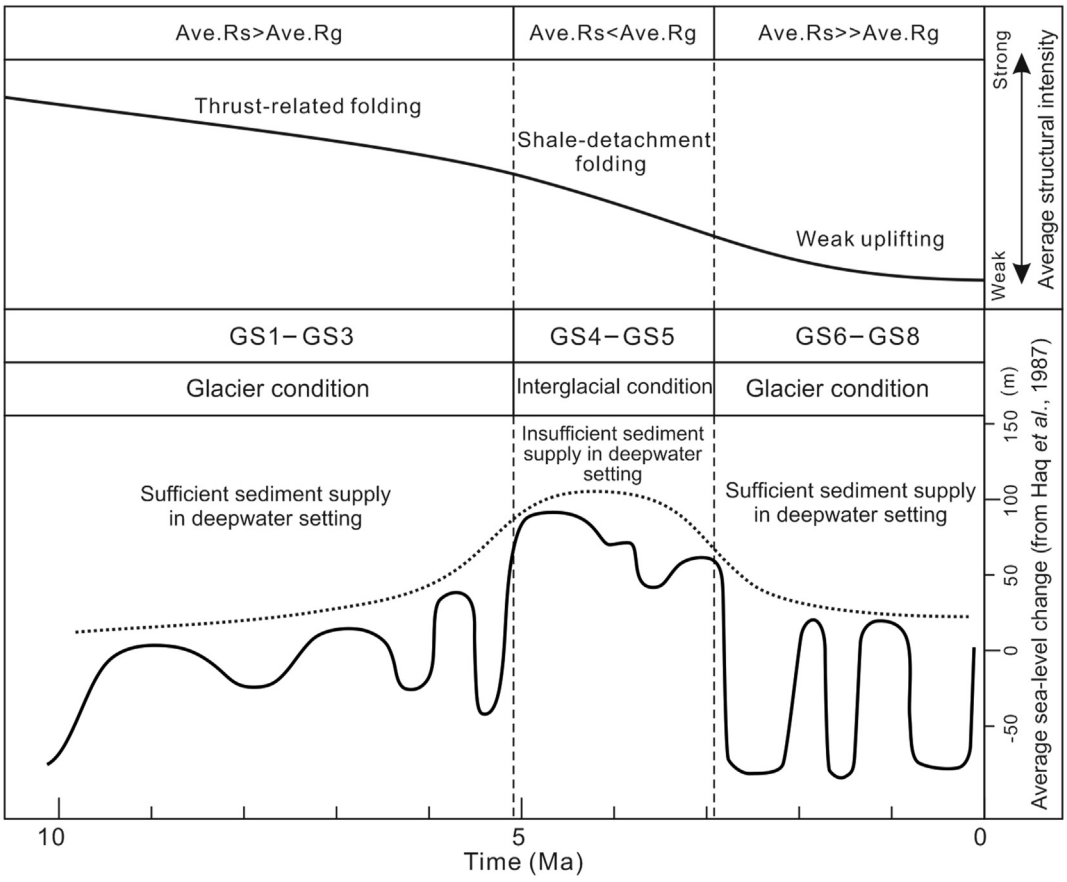

Fig. 11 Interaction relationship between structural activities and sea-level changes (refer to Haq *et al.*, 1987; Zhang *et al.*, 2021) during the formation of different growth sequences (GS1—GS8). Ave. Rs = Average sedimentation rate; Ave. Rg = Average structural growth rate.

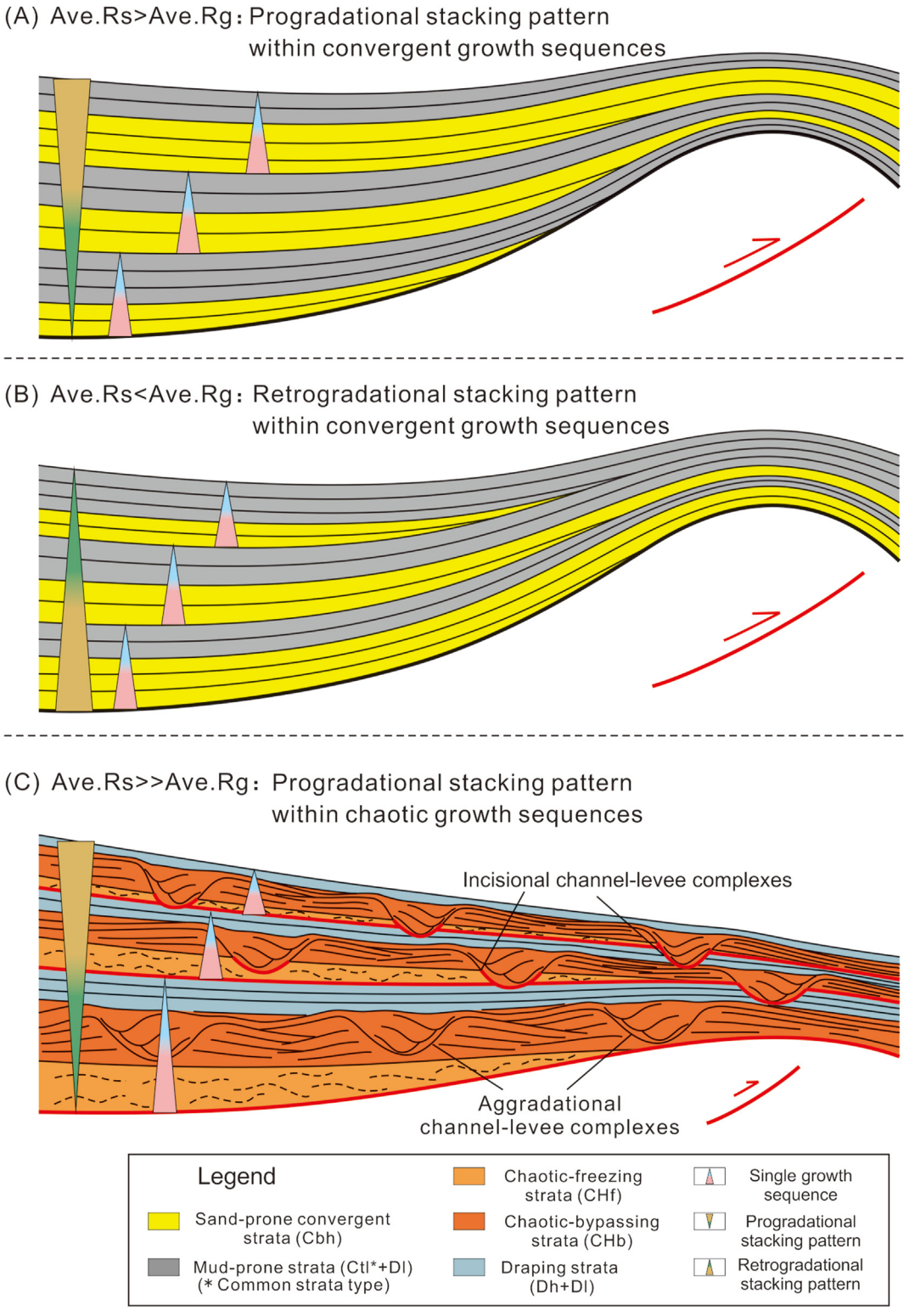

Fig. 12 Schematic illustration for the stacking patterns within growth sequences. **A)** Progradational stacking pattern within convergent growth sequences; **B)** Retrogradational stacking pattern within convergent growth sequences; **C)** Progradational stacking pattern within chaotic growth sequences. Ave. Rs = Average sedimentation rate; Ave. Rg = Average structural growth rate.

lack accurate sediment dating, we assume that a single falling—rising cycle of sea level is likely to have led to the formation of the single growth sequence, considering the close relationship between seal—level cycles and growth sequences since ca. 9.5 Ma.

Corresponding to the three stages of sea-level change, the gravitational deformation in the study area was also dominated by different structural activities with gradually decreasing growth rate (Fig. 11, Zhang *et al.*, 2021), which controlled the change of accommodation space. The accommodation space relative to sediment supply, i.e., the A/S ratio of intraslope basins, may change through time, leading to varying ratio of strata units within growth sequences (Table 2; Fig. 9). The ratio of Cbh strata within a single convergent growth sequence, which represents high-energy deposition at low stands of sea level, potentially reflects the A/S ratio of intraslope basins. In cases with higher A/S ratio, the average sedimentation rate could be lower than the average structural growth rate, resulting in the under-filling state of basins indicated by low ratio of Cbh, such as GS1. Whereas in cases with lower A/S ratio, the average sedimentation rate could be larger than the average structural growth rate, resulting in the over-filling state of basins indicated by large ratio of Cbh, such as GS3. Moderate A/S suggests a balance between the sedimentation rate and the structural growth rate, resulting in a balanced filling state of basins indicated by the moderate ratio of Cbh, such as GS2.

The variations of A/S between growth sequences are generally controlled by the interaction between sea-level cycles and gravitational deformation, which resulted in three strata stacking patterns corresponding to the three sedimentary—tectonic interacting stages (Figs. 11 and 12). The first stage (deposition of GS1—GS3) is characterized by dominant thrust-related folding with high structural growth rate (Fig. 11), which resulted in the large ponded-basin accommodation space filled with convergent growth sequences (Fig. 9). The sedimentation rate during this period is overall high driven by glaciation sea-level cycle. Gradual weakening of thrust-related folding from GS1 to GS3 resulted in an upward decrease in the A/S of intraslope basins, and the ratio of Cbh strata units (high-energy deposition) decreased upwards accordingly, representing a progradational stacking pattern within convergent growth sequences (Fig. 12A). The second stage (deposition of GS4—GS5) is characterized by dominant detachment folding with moderate structural growth rate (Fig. 11). The average sedimentation rate under deglaciation sea-level change is overall lower than the average structural growth rate, resulting in the upward-increasing A/S within intraslope basins (Figs. 8—10). This trend is indicated by the upward decrease in the ratio of Cbh strata units, representing a retrogradational stacking pattern within convergent growth sequences (Fig. 12B). The third stage (deposition of GS6—GS8) is characterized by the low structural growth rate that is far outpaced by the high sedimentation rate induced by glaciation sea-level cycles (Fig. 11). The intraslope basins during this period were dominated by slope accommodation space filled with chaotic strata. As the A/S of intraslope basins decreased rapidly, the chaotic-bypassing (CHb) strata evolved from dominant depositional channels to dominant incisional channels (Fig. 9), representing a progradational pattern within chaotic growth sequences (Fig. 12C).

Under common conditions from regional gravitational contraction and global sea-level change, similar growth sequence characteristics with varying stratigraphic architecture have been recognized in other deep-water regions of the Niger Delta Basin (Maloney *et al.*, 2010; Jolly *et al.*, 2016; Chima *et al.*, 2019, 2020). The minor difference lies in the starting time of growth sequences because of different structural histories from place to place. Overall, the growth strata patterns presented here can be representative of the entire deep-water Niger Delta Basin, and may also apply to all the thrust-related intraslope basins with shale detachment styles.

7. Conclusions

This study provides an example of thrust-related intraslope basins that were filled by growth sequences with varying stratigraphic architecture. Analysis of the 3D seismic data recognized three types of growth strata units: convergent, draping, and chaotic. The convergent strata units were mainly filled in the ponded-basin accommodation space produced by thrust-related folding. The filling succession of a single convergent growth sequence generally began with convergent-baselapping strata succeeded by convergent-thinning strata and draping strata, which represents ponded-to-bypass transition taking place in the ponded-basin accommodation space. A dynamic fill-and-spill model is proposed to explain the formative mechanism of convergent growth sequence architecture, which considers the relationship between episodic sedimentation rate and structural growth rate. The glaciation or deglaciation sea-level cycles interacted with the gravitational deformation would result in a progradational or retrogradational stacking pattern within convergent growth sequences. As the gravitational deformation became weak, intraslope

basins were dominated by the slope accommodation space filled with chaotic strata units. The filling succession of a single chaotic growth sequence began with chaotic-freezing strata of debris flows succeeded by chaotic-bypassing strata of turbidite channel-levees, reflecting dominant erosion-bypassing processes taking place in the slope accommodation space. With the structural growth rate exceeded by the high sedimentation rate under glaciation sea-level change, the slope accommodation space decreased rapidly, resulting in a progradational stacking pattern within chaotic growth sequences. This study highlights the sedimentary—tectonic interaction on the growth sequence architecture in a deep-water gravitational system, and improves our understandings of thrust-related intraslope basins that have complex stratigraphic patterns at a variety of scales.

Funding

This study is funded by the National Natural Science Foundation of China (Grant Nos. 42002112, 42272110), the Strategic Cooperation Technology Projects of China National Petroleum Corporation (CNPC) and China University of Petroleum (Beijing) (Grant No. ZLZX2020-02), and the Science Foundation for Youth Scholars of China University of Petroleum (Beijing) (Grant No. 2462022BJRC006).

Availability of data and materials

The data that support the findings of this study are available on request from the corresponding author.

Authors' contributions

All the authors have actively participated in the preparation of the manuscript. Jia—Jia Zhang devised the conceptual idea, wrote much of the paper, and outlined the figures. Sheng-He Wu, Guang-Yi Hu and Da-Li Yue provided constructive suggestions and made careful editing on the manuscript. Cheng Chen, Mei Chen, Ji-Tao Yu, Qi-Cong Xiong and Li-Qiong Wang supported seismic data interpretation. All authors read and approved the final proof.

Conflicts of interest

The authors declare that they have no known competing financial interests or personal relationships that could have appeared to influence the study reported in this paper.

Acknowledgements

We thank the China National Offshore Oil Corporation (CNOOC) for providing and permitting publication of the subsurface data. We would like to thank our colleagues, Zi-Hao Liu, Zhen-Hua Xu, Ke Zhang, and Jun-Jie Wang for their help with seismic data interpretation and data analyses.

References

Beaubouef, R.T., Friedmann, S.J., 2000. *High resolution seismic sequence stratigraphic framework for the evolution of Pleistocene intra slope basins, western Gulf of Mexico: Depositional models and reservoir analogs // Deep-water reservoirs of the world*. Gulf Coast Section SEPM 20th Annual Research Conference, pp. 40—60.

Briggs, S.E., Davies, R.J., Cartwright, J.A., Morgan, R., 2006. Multiple detachment levels and their control on fold styles in the compressional domain of the deep-water west Niger Delta. *Basin Research*, 18, 435—450.

Brown Jr., L.F., Loucks, R.G., Trevio, R.H., Hammes, U., 2004. Understanding growth-faulted, intraslope subbasins by applying sequence-stratigraphic principles: Examples from the south Texas Oligocene Frio Formation. *AAPG Bulletin*, 88(11), 1501—1522.

Brun, J.P., Fort, X., 2004. Compressional salt tectonics (Angolan Margin). *Tectonophysics*, 382, 129—150.

Chima, K.I., Do Couto, D., Leroux, E., Gardin, S., Hoggmascall, N., Rabineau, M., Granjeon, D., Gorini, C., 2019. Seismic stratigraphy and depositional architecture of Neogene intraslope basins, offshore western Niger Delta. *Marine and Petroleum Geology*, 109, 449—468.

Chima, K.I., Gorini, C., Rabineau, M., Granjeon, D., Do Couto, D., Leroux, E., Hoggmascall, N., 2020. Pliocene and Pleistocene stratigraphic evolution of the western Niger Delta intraslope basins: A record of glacio-eustatic sea-level and basin tectonic forcings. *Global and Planetary Change*, 195, 103355.

Clark, I.R., Cartwright, J.A., 2011. Key controls on submarine channel development in structurally active settings. *Marine and Petroleum Geology*, 28(7), 1333—1349.

Clark, I.R., Cartwright, J.A., 2012. *Interactions between Coeval Sedimentation and Deformation from the Niger Delta Deep-Water Fold Belt*, vol. 99. SEPM Special Publication, pp. 243—267.

Cohen, H.A., McClay, K., 1996. Sedimentation and shale tectonics of the northwestern Niger Delta front. *Marine and Petroleum Geology*, 13, 313—328.

Corredor, F., Shaw, J.H., Bilotti, F., 2005. Structural styles in the deep-water fold and thrust belts of the Niger Delta. *AAPG Bulletin*, 89, 753—780.

Curry, M.A.E., Peel, F.J., Hudec, M.R., Norton, I.O., 2018. Extensional models for the development of passive-margin salt basins, with application to the Gulf of Mexico. *Basin Research*, 30, 1180—1199.

Damuth, J.E., Olson, H.C., 2015. Latest Quaternary sedimentation in the northern Gulf of Mexico Intraslope Basin Province: I. Sediment facies and depositional processes. *Geosphere*, 11(6), 1689—1718.

Deptuck, M.E., Piper, D.J.W., Savoye, B., Gervais, A., 2008. Dimensions and architecture of late Pleistocene submarine lobes off the northern margin of East Corsica. *Sedimentology*, 55(4), 869—898.

Duerto, L., McClay, K., 2011. Role of the shale tectonics on the evolution of the Eastern Venezuelan Cenozoic thrust and fold belt. *Marine and Petroleum Geology*, 28, 81—108.

Galindo, P.A., Lonergan, L., 2020. Basin evolution and shale tectonics on an obliquely convergent margin: The Bahia Basin, Offshore Colombian Caribbean. *Tectonics*, 39, e2019TC005787.

Gee, M.J.R., Gawthorpe, R.L., 2006. Submarine channels controlled by salt tectonics: Examples from 3D seismic data offshore Angola. *Marine and Petroleum Geology*, 23, 443—458.

Gong, C.L., Steel, R.J., Wang, Y.M., Lin, C.S., Olariu, C., 2016. Shelf-margin architecture variability and its role in sediment-budget partitioning into deep-water areas. *Earth-Science Reviews*, 154, 72—101.

Haq, B.U., Hardenbol, J., Vail, P.R., 1987. Chronology of fluctuating sea levels since the Triassic. *Science*, 235, 1156—1166.

Janocko, M., Nemec, W., Henriksen, S., Warchoł, M., 2013. The diversity of deep-water sinuous channel belts and slope valley-fill complexes. *Marine and Petroleum Geology*, 41, 7—34.

Jolly, B.A., Lonergan, L., Whittaker, A.C., 2016. Growth history of fault-related folds and interaction with seabed channels in the toe-thrust region of the deep-water Niger Delta. *Marine and Petroleum Geology*, 70, 58—76.

Jolly, B.A., Whittaker, A.C., Lonergan, L., 2017. Quantifying the geomorphic response of modern submarine channels to actively growing folds and thrusts, deep-water Niger Delta. *GSA Bulletin*, 129, 1123—1139.

Kopriva, B.T., Kim, W., 2015. Coevolution of minibasin subsidence and sedimentation: Experiments. *Journal of Sedimentary Research*, 85(3), 254—264.

Lamb, M.P., Toniolo, H., Parker, G., 2006. Trapping of sustained turbidity currents by intraslope minibasins. *Sedimentology*, 53(1), 147—160.

Li, L., Wang, Y.M., Zhang, L.M., Huang, Z.C., 2010. Confined gravity flows sedimentary process and its impact on the lower continental slope, Niger Delta. *Science China Earth Sciences*, 40(11), 1591—1597.

Madof, A.S., Christie-Blick, N., Anders, M.H., 2009. Stratigraphic controls on a salt-withdrawal intraslope minibasin, north-central Green Canyon, Gulf of Mexico: Implications for misinterpreting sea level change. *AAPG Bulletin*, 93(4), 535—561.

Maloney, D., Davies, R., Imber, J., Higgins, S., King, S., 2010. New insights into deformation mechanisms in the gravitationally driven Niger Delta deep-water fold and thrust belt. *AAPG Bulletin*, 94, 1401—1424.

Mchargue, T., Pyrcz, M.J., Sullivan, M.D., Clark, J.D., Fildani, A., Romans, B.W., Covault, J.A., Levy, M., Posamentier, H.W., Drinkwater, N.J., 2011. Architecture of turbidite channel systems on the continental slope: Patterns and predictions. *Marine and Petroleum Geology*, 28(3), 728—743.

Pizzi, M., Lonergan, L., Whittaker, A.C., Mayall, M., 2020. Growth of a thrust fault array in space and time: An example from the deep-water Niger Delta. *Journal of Structural Geology*, 137, 104088.

Postma, G., Nemec, W., Kleinspehn, K.L., 1988. Large floating clasts in turbidites, a mechanism for their emplacement. *Sedimentary Geology*, 58, 47—61.

Prather, B.E., Booth, J.R., Steffens, G.S., Craig, P.A., 1998. Classification, lithologic calibration, and stratigraphic succession of seismic facies of intraslope basins, deep-water Gulf of Mexico. *AAPG Bulletin*, 82(5), 701—728.

Prather, B.E., Pirmez, C., Winker, C.D., 2012. Stratigraphy of linked intraslope basins: Brazos-Trinity system western Gulf of Mexico. In: *Application of the Principles of Seismic Geomorphology to Continental-Slope and Base-of-Slope Systems: Case Studies from Seafloor and Near-Seafloor Analogues*, vol. 99. SEPM Special Publication, pp. 83—109.

Suppe, J., 1985. *Principles of Structural Geology*. Prentice Hall, Englewood Cliffs, New Jersey, pp. 280—307.

Sylvester, Z., Cantelli, A., Pirmez, C., 2015. Stratigraphic evolution of intraslope minibasins: Insights from surface-based model. *AAPG Bulletin*, 99, 1099—1129.

Uchupi, E., 1989. The tectonic style of the Atlantic Mesozoic rift system. *Journal of African Earth Sciences*, 8, 143—164.

Wu, J., Mcclay, K., Frankowicz, E., 2015. Niger Delta gravity-driven deformation above the relict Chain and Charcot oceanic fracture zones, Gulf of Guinea: Insights from analogue models. *Marine and Petroleum Geology*, 65, 43—62.

Zecchin, M., Catuneanu, O., 2013. High-resolution sequence stratigraphy of clastic shelves I: Units and bounding surfaces. *Marine and Petroleum Geology*, 39, 1—25.

Zhang, J.J., Gulick, S.P.S., 2020. Sequence stratigraphy and depositional history of the baranof fan: Insights for cordilleran ice sheet outflow to the Gulf of Alaska. *GSA Bulletin*, 132(1—2), 353—372.

Zhang, J.J., Wu, S.H., Hu, G.Y., Yue, D.L., Xu, Z.H., Chen, C., Zhang, K., Wang, J.J., Wen, S.Y., 2021. Role of shale deformation in the structural development of a deep-water gravitational system in the Niger Delta. *Tectonics*, 40, e2020TC006491.